2011 American Control Conference
on O'Farrell Street, San Francisco, CA, USA
June 29 - July 01, 2011

Performance Metrics for Fault Detection and Isolation Filters

Rohit Pandita[†], József Bokor[♮] and Gary Balas[♯]

Abstract— **Fault detection and isolation (FDI) filters are typically synthesized for open-loop or closed-loop systems. The controller affects the FDI filter performance in the closed-loop. Performance metrics for FDI filters are proposed to assess filter performance and controller-filter interaction in the presence of uncertain dynamics in the closed-loop. The role of controller's robustness to plant uncertainty in FDI filter performance is examined.**

I. INTRODUCTION

Safety critical systems like flight control system (FCS) require redundancy to guarantee fail-operational or fail-safe functionality. Model-based fault diagnosis filters make use of a dynamic model of the system to identify and isolate faults. A survey of the model-based fault diagnosis methods can be found in [4], [9], [11]. Commonly, engineers synthesize feedback controllers independent of the fault detection filters. The model used for fault detection and isolation (FDI) filter design is often based on the open-loop system. The drawback of the independent filter/controller synthesis approach is the assumption that plant dynamics are precisely known, which is seldom the case in practical applications. FDI filters designed independently may suffer from poor performance, missed detections, false alarms, etc, due to coupling of the plant, controller and model errors of the system. Stoustrup et al., [22] showed that in the presence of plant uncertainty the controller and FDI filter design are coupled, hence the design of the filter depends on the controller. An optimal design cannot be obtained without considering the controller and FDI filter design problem simultaneously. This approach is known as the *integrated FDI filter design problem*. Uncertainty in the system model is inevitable in real-world control engineering problems including aircraft flight control. It is unknown how close to *optimal* the FDI filter can achieve when it is designed separately from the flight control system. Hence, it is imperative to better understand the interaction between the closed-loop system and the FDI filter in the presence of uncertainty.

Irrespective of the technique used to design an FDI filter, the basic requirements are typically the following - Capability to isolate faults that occur simultaneously, sensitivity to a particular fault and insensitivity to other faults, robustness to modeling uncertainty, good attenuation of external disturbances and noise at the FDI filter output, asymptotic convergence of the FDI filter output to a non-zero steady-state in response to a non-zero fault, zero output otherwise.

The term *metric* is used in the sense of a quantitative measure of the figure-of-merit or goodness of FDI filter performance. The goal of this paper is to present an engineering application of the FDI metrics described in [21]. To show the versatility of the metrics, two FDI filters are synthesized using different techniques for comparison. The proposed metrics are used to assess the benefits of the individual FDI filters on the closed-loop systems with model uncertainty. The key component used to assess the influence of the closed-loop controller on filter performance is the output sensitivity function (S) and helps to illustrate the design trade-offs between the filter and the controller.

The FDI performance metrics are applied to a flight control example associated with the NASA Generic Transport Model (GTM), [5], [14] longitudinal axis dynamics. FDI filters are synthesized to estimate a sensor and an actuator fault using two approaches, the $\mathcal{H}_\infty$ model matching and the geometric design technique. The $\mathcal{H}_\infty$ model matching design, [6], [13], [17], [21], [23], is a closed-loop design problem in which knowledge of the tracking controller is exploited in filter synthesis. The geometric filter design technique, [3], [18], is an open-loop filter design technique that exploits the invariant subspaces of the state-space.

The paper is organized as follows, the first section revisits development of the closed-loop FDI filter performance metrics provided in [21]. The NASA GTM aircraft longitudinal dynamics are described, including the dynamic uncertainty model used. The sensor and actuator faults used in the problem are explained. The FDI performance metrics are applied to the two dissimilar FDI filters synthesized for this uncertain plant. The results obtained using the metrics are discussed. The positive influence controller robustness on FDI filter performance is highlighted.

II. PROBLEM STATEMENT AND ANALYSIS

Input-output properties of the FDI filter and closed-loop system are derived in this section. The plant model is assumed to be a linear time-invariant (LTI) system and described by a state-space model,

$$\dot{x}(t) = Ax(t) + Bu(t) \tag{1a}$$
$$y(t) = Cx(t) + Du(t) \tag{1b}$$

where, $x \in \mathbb{R}^n$, $u \in \mathbb{R}^p$, $y \in \mathbb{R}^m$ are the states, controls and measurements, respectively, and A, B, C and D are real matrices of the corresponding dimension. Let $G(s) =$

[†]Graduate Research Assistant, Department of Aerospace Engineering and Mechanics, University of Minnesota, Minneapolis, MN 55455, USA, pandi008@umn.edu

[♯]Professor and Head, Department of Aerospace Engineering and Mechanics, University of Minnesota, Minneapolis, MN 55455, USA, balas@aem.umn.edu

[♮]Head, Systems and Control Laboratory, Computer and Automation Research Institute of the Hungarian Academy of Sciences H-1111 Budapest, Kende u. 13-17, K-211, Hungary, bokor@sztaki.hu

$C(sI-A)^{-1}B+D$ be the transfer function representation of the linear plant model.

Model uncertainty is captured through a general class of uncertain plants, $G_\Delta(s)$, where $\Delta(s) := \{\mathbf{\Delta} : \Delta \in \mathbb{C}_{m\times m}, \bar{\sigma}(\Delta) \leq 1\}$, is a complex norm bounded uncertainty with arbitrary phase. This general description can include multiplicative, additive, linear fractional transformation (LFT) or other types of uncertain plant models, [8].

The fault estimation and tracking control problem is formulated as shown in Fig. 1(a). Sensor faults, f_s and actuator faults, f_a are assumed to enter in an additive manner. Weights, $W_a(s)$ and $W_s(s)$, describe the frequency content of actuator and sensor faults respectively and are in general block diagonal matrices for multi-input/multi-output (MIMO) systems. $W_a(s)$ and $W_s(s)$ are assumed to be known functions derived from fault modeling, and their development is not discussed in this paper. See [2], [15] for information regarding the development of fault weighting functions. Weighting functions $W_{p_f}(s)$ and $W_{p_c}(s)$ are design parameters used to shape the desired controller and FDI filter performance objectives.

A standard model matching $\mathcal{H}_\infty$ synthesis technique is used to design a filter and controller. The design objective is to minimize the gain of the transfer function matrix from faults ($f = \begin{bmatrix} f_a & f_s \end{bmatrix}^T$) and tracking reference (y_c) to weighted fault estimation error ($\tilde{e}_f$) and weighted reference tracking error ($\tilde{e}_c$), respectively, measured in terms of the $\mathcal{H}_\infty$ norm of the closed-loop system. The synthesis problem is convex and many algorithms are available in the literature to solve for the optimal $\mathcal{H}_\infty$ controllers [7], [10].

The $\mathcal{H}_\infty$ problem formulation feeds the measurements ($m \times 1$) and tracking reference vector ($q \times 1$) separately to the controller-filter $K(s)$ which is to be designed. The outputs of $K(s)$ are the control inputs, u_c, and the fault estimation vector, $u_f = \begin{bmatrix} \hat{f}_a & \hat{f}_s \end{bmatrix}^T$. $\hat{f}_a$ and $\hat{f}_s$ are estimates of actuator and sensor faults, respectively. The input-output topology allows $K(s)$ to be partitioned into four components as shown in Eq. 2. This is known as the *four-parameter controller-filter problem* in the literature, [12], [19], [22]. The controller-filter partitions are,

$$K(s) = \left[\begin{array}{c|c} K_{c_1}(s) & K_{c_2}(s) \\ \hline K_{f_1}(s) & K_{f_2}(s) \end{array}\right] \tag{2}$$

and the input-output signals for $K(s)$ are,

$$\begin{pmatrix} u_c \\ u_f \end{pmatrix} = K(s) \begin{pmatrix} y_m \\ y_c \end{pmatrix}$$

The elements $K_{c_1}(s)$ and $K_{f_1}(s)$ are the feedback components of the tracking controller and the filter, respectively, which act on the measurements, y_m. The elements $K_{c_2}(s)$ and $K_{f_2}(s)$ are the feed-forward elements, respectively.

Consider the open-loop equations for the interconnection shown in Fig. 1(a),

$$\begin{aligned} \tilde{e}_c &= W_{p_c}(s)[y_c - G_\Delta(s)(u_c + W_a(s)f_a) - W_s(s)f_s] && \text{(3a)} \\ \tilde{e}_f &= W_{p_f}(s)\left(u_f - \begin{bmatrix} W_a(s)f_a \\ W_s(s)f_s \end{bmatrix}\right) && \text{(3b)} \\ y_m &= -(G_\Delta(s)[u_c + W_a(s)f_a] + W_s(s)f_s) && \text{(3c)} \end{aligned}$$

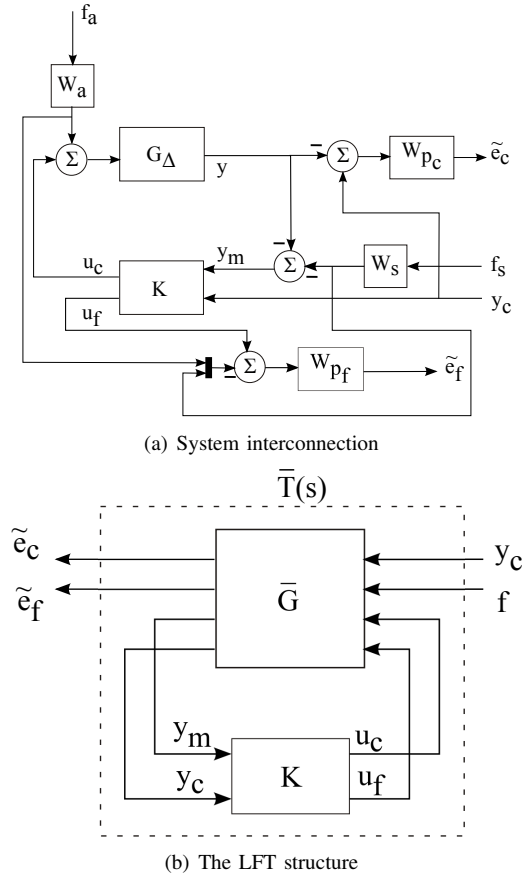

(a) System interconnection

(b) The LFT structure

Fig. 1. Fault estimation filter and tracking control problem

The system of equations in Eq. 3 (a)-(c) describing the open-loop input-output signals can be rewritten in a matrix form as,

$$\begin{bmatrix} \tilde{e}_c \\ \tilde{e}_f \\ y_m \\ y_c \end{bmatrix} = \underbrace{\left[\begin{array}{ccc|cc} W_{p_c} & -W_{p_c}\begin{bmatrix} G_\Delta W_a & W_s \end{bmatrix} & & -W_{p_c}G_\Delta & 0 \\ 0 & -W_{p_f}\begin{bmatrix} W_a & 0 \\ 0 & W_s \end{bmatrix} & & 0 & W_{p_f} \\ \hline 0 & -\begin{bmatrix} G_\Delta W_a & W_s \end{bmatrix} & & -G_\Delta & 0 \\ I & 0 & & 0 & 0 \end{array}\right]}_{\bar{G}(s)} \begin{bmatrix} y_c \\ f \\ u_c \\ u_f \end{bmatrix} \tag{4}$$

where, $f = \begin{bmatrix} f_a & f_s \end{bmatrix}^T$, is the augmented fault vector. Introducing the controller-filter $K(s)$ to form the lower LFT structure as shown in Fig. 1(b) and simplifying system equations, the closed-loop transfer matrix, $\bar{T}(s)$, can be obtained,

$$\begin{bmatrix} \tilde{e}_c \\ \tilde{e}_f \end{bmatrix} = \bar{T}(s) \begin{bmatrix} y_c \\ f \end{bmatrix} \tag{5}$$

where $\bar{T}(s)$ is block partitioned as,

$$\bar{T}(s) = \begin{bmatrix} \bar{T}_{11} & \bar{T}_{12} \\ \bar{T}_{21} & \bar{T}_{22} \end{bmatrix} \tag{6}$$

and the elements of matrix $\bar{T}(s)$ are given as follows,

$$\begin{aligned} \bar{T}_{11} &= W_{p_c}[I - S_\Delta G_\Delta K_{c_2}] && \text{(7a)} \\ \bar{T}_{12} &= -W_{p_c}(I - T_\Delta)\begin{bmatrix} G_\Delta W_a & W_s \end{bmatrix} && \text{(7b)} \\ \bar{T}_{21} &= -W_{p_f}(K_{f_1}S_\Delta G_\Delta K_{c_2} - K_{f_2}) && \text{(7c)} \\ \bar{T}_{22} &= -W_{p_f}\left(K_{f_1}S_\Delta\begin{bmatrix} G_\Delta W_a & W_s \end{bmatrix} - \begin{bmatrix} W_a & 0 \\ 0 & W_s \end{bmatrix}\right) && \text{(7d)} \end{aligned}$$

where, the output complementary sensitivity and the output sensitivity function are given by,

$$T_\Delta = G_\Delta K_{c_1}(I + G_\Delta K_{c_1})^{-1}, S_\Delta = (I + G_\Delta K_{c_1})^{-1} \quad (8)$$

The $\mathcal{H}_\infty$ controller and filter synthesis, is carried out, either simultaneously or independently, by minimizing the maximum singular value of the transfer function matrix $\bar{T}(s)$ over the set of permissible controllers/filters.

III. METRICS FOR FDI FILTER AND CONTROLLER INTERACTION

The transfer function matrices obtained in Eq. 7 (a)-(d) offer valuable insights into the closed-loop behavior of FDI filters [21]. These transfer matrices can also be used to define performance metrics for FDI filters. Consider Eq. 7(d), based on problem setup shown in Fig. 1(a) and Eq. 5. The filter parameter $K_{f_1}(s)$ can be further block partitioned as,

$$K_{f_1}(s) = \begin{bmatrix} K^a_{f_1}(s) \\ K^s_{f_1}(s) \end{bmatrix} \quad (9)$$

Eq. 7(d) is the transfer function matrix from faults (f) to weighted fault estimation error ($\tilde{e}_f$),

$$\begin{bmatrix} \tilde{e}_{f_a} \\ \tilde{e}_{f_s} \end{bmatrix} = \bar{T}_{22}(s) \begin{bmatrix} f_a \\ f_s \end{bmatrix}$$

Using Eq. 7(d) and Eq. 9, and removing the weighting functions,

$$\begin{pmatrix} e_{f_a} \\ e_{f_s} \end{pmatrix} = \begin{bmatrix} K^a_{f_1} S_\Delta G_\Delta - I & K^a_{f_1} S_\Delta \\ K^s_{f_1} S_\Delta G_\Delta & K^s_{f_1} S_\Delta - I \end{bmatrix} \begin{pmatrix} f_a \\ f_s \end{pmatrix} \quad (10)$$

Thus, given the closed-loop controller, $K_c(s)$, the uncertain plant model, $G_\Delta(s)$ and the FDI filter, $K_f(s)$, the transfer matrix in Eq. 10 is completely known. A closer look at each term in this transfer matrix reveals

- The diagonal terms in Eq. 10 are the fault signals to fault estimation error transfer functions. The transfer function $(K^a_{f_1} S_\Delta G_\Delta - I)$ maps the actuator fault to the actuator fault estimation error. Similarly, $(K^s_{f_1} S_\Delta - I)$ maps the sensor fault to the senor fault estimation error. For an ideal FDI filter, it is expected that the gain of these two transfer functions is zero, implying that the FDI filter can perfectly estimate fault signals across frequency.
- The off-diagonal terms in Eq. 10 represent fault cross-coupling, that is, an actuator fault showing up in sensor fault estimate signal/residual, and vice-versa. Ideally, the two transfer functions, $K^a_{f_1} S_\Delta$ and $K^s_{f_1} S_\Delta G_\Delta$ should be as close to zero as possible, a property referred to in the literature as *fault-isolation*.

The worst-case fault estimation error of the FDI filter in the presence of $\Delta(s)$ uncertainty can be founded by evaluating the worst-case gain of each of the four blocks of the transfer function matrix in Eq. 10. These form the basis for the metrics to assess FDI filter performance. A large worst-case gain would indicate degradation of the FDI filter closed-loop performance in the presence of model uncertainty. Packard et al., [20] describe a method to compute the worst-case gain of any uncertain transfer function. The worst-case gain function, *wcgain*, in the MATLAB *Robust Control Toolbox*, [1] exploits this method and is used in the examples presented in later sections to compute the metrics. The actuator fault estimation metric can be computed as,

$$\max_{\Delta \in \mathbf{\Delta}} \quad \| K^a_{f_1} S_\Delta G_\Delta - I \|_\infty \quad (11)$$

and the corresponding sensor fault estimation metric as,

$$\max_{\Delta \in \mathbf{\Delta}} \quad \| K^s_{f_1} S_\Delta - I \|_\infty \quad (12)$$

IV. APPLICATION OF FAULT DETECTION METRICS

Application of the metrics proposed in Sec. III to a flight control example problem is presented in this section. Two FDI filters are designed, one based on the geometric technique, [3], [18] and one $\mathcal{H}_\infty$ FDI filter, [16], [21] to provide a distinct pair of test-filters. An identical pitch command tracking controller, $K_c(s)$, is used with both the test filters as a benchmark.

A. NASA GTM closed-loop longitudinal dynamics

The NASA Generic Transport Model (GTM) is a 5.5% scale model replica of a typical twin turbofan powered commercial airliner, which was designed as a platform for flight safety related research and experiments, [5], [14].The GTM nonlinear model is trimmed in a straight-and-level flight condition at True Airspeed (TAS) = 90 knots. A linearized longitudinal model is obtained at this equilibrium.

Uncertainty Modeling:

An input multiplicative uncertainty model is proposed to over-bound the set of plant models at different equilibrium states in the flight envelope. A model of the form $G_\Delta(s) = G(s)(I + \Delta(s)W_u(s))$, $\bar{\sigma}(\Delta(s)) \leq 1$ is obtained, where $W_u(s)$ is the uncertainty weighting function.

A pitch attitude command/reference tracking controller is designed using $\mathcal{H}_\infty$ model-matching techniques. The GTM plant outputs used for feedback are: pitch attitude (θ, rad), pitch-rate (q, rad/s), airspeed (TAS, knots) and angle-of-attack (α, rad). The control input is elevator deflection (δ_e, rad).

B. Sensor and actuator fault description

Two faults are selected for the synthesis of FDI filter, one sensor and one actuator fault. The pitch-rate gyro is chosen as a faulted sensor. The GTM longitudinal model has only one input, the elevator, which is selected as the actuator fault channel.

In general, multiple failure modes exist for the pitch-rate gyro and the elevator, for example, a fault in the pitch-rate gyro can manifest itself as a null-shift, zero-output (dead-sensor) or scale-factor error. Similarly, the elevator fault can manifest itself as a locked-elevator, a hard-over failure, floating elevator, etc. Two failure modes are considered in this work, the null-shift and the floating failure mode. The null-shift is classified as a change in zero position of the

sensor/actuator. The floating failure implies that the output (sensor output or actuator position) floats (oscillates) between two arbitrary values.

C. Application of filter performance metrics

In the example, two FDI filters are compared with respect to each other using the proposed filter metrics. The GTM longitudinal model with multiplicative input uncertainty and the $\mathcal{H}_\infty$ pitch controller described in previous section comprise the set of closed-loop systems. The FDI filter designs considered are:

1) Filter 1: Geometric filter design, [3], [18] with five inputs, namely, the four measured states, airspeed, angle-of-attack, pitch-rate and pitch angle, and one plant input, the elevator deflection. The filter is designed to have stable residual dynamics, i.e., filter output (residual) asymptotically converges to zero when no fault is present.
2) Filter 2: $\mathcal{H}_\infty$ fault estimation filter design with the same five measurements as above.

The worst-case actuator and sensor fault estimation metrics given in Sec. III are computed using *wcgain* which computes the worst-case gain of an uncertain transfer function (performance metrics in this case) at each frequency point as shown in Fig. 2 and also returns the corresponding $\Delta(s)$ uncertainty that results in the worst gain, at each frequency. The metrics predict the filters will have very good steady-state performance, indicated by a small value (close to zero) of the metric in the low frequency range. Also, at high frequency both sensor and actuator fault metrics settle at unity gain. As seen from the sensor and actuator fault metrics obtained in Sec. III, unity gain of the two metrics at high frequency is a consequence of $K^s_{f_1}(s)S_\Delta(s) \to 0$, $K^a_{f_1}(s)S_\Delta(s)G_\Delta(s) \to 0$, as $s \to \infty$, respectively. This is due to the filter *roll-off* which results in its inability to detect/estimate high frequency sensor and actuator faults.

Consider the worst-case filter performance as predicted by the metrics in Fig. 2 (a),(b) at the frequency of 1 rad/s. Both the filters are compared at that specific frequency point using the worst-case linear time-domain simulation in Fig. 3 and 4. The time domain simulation is obtained by first substituting the worst-case $\Delta(s)$ uncertainty obtained from the worst-case gain computation of the two metrics, respectively, into the multiplicative uncertainty model of GTM longitudinal dynamics, $G_\Delta(s)$. Two test cases are investigated, one compares the sensor fault estimation performance in which a 1 deg/s peak amplitude sinusoidal gyro fault is injected at 1 rad/s, Fig. 3. Note the measurement unit of angular rotation rate is deg/s. This may be confused with the frequency of fault variation, given in rad/s . The other compares actuator fault estimation performance by injecting a sinusoidal elevator fault of 1 deg peak magnitude at 1 rad/s frequency as shown in Fig. 4.

The actuator fault metric at 1 rad/s for the two filters is close to zero in Fig. 2(a), indicating that both the filters should perform equally well for a 1 deg elevator fault. This is consistent with the time-domain simulation results seen in

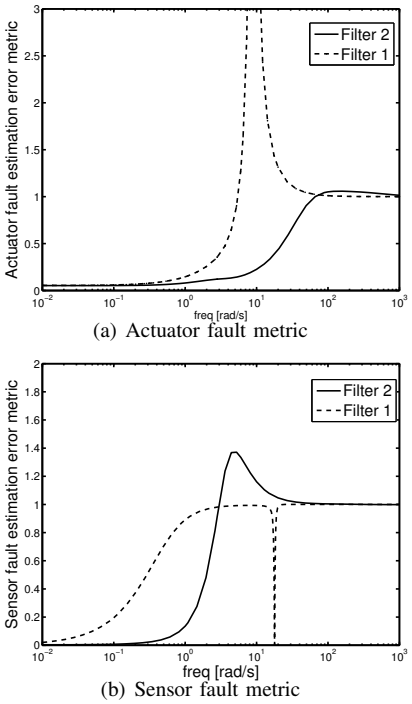

(a) Actuator fault metric

(b) Sensor fault metric

Fig. 2. Comparison of fault estimation error metrics for four different FDI filters

Fig. 3 where both the filters are able to track a 1 deg peak elevator fault with very little error. Similarly, comparing the sensor fault metric at 1 rad/s for the two filters in Fig. 2(b) it may be noted that the value of the metric for the Filter 1 is much higher than that for Filter 2, hence Filter 2 is expected to perform better in this test. This assessment is also consistent with the worst-case time-domain simulation seen in Fig. 4, in which the worst-case performance for Filter 1 is seen to have much larger steady state error in gyro fault estimate compared to Filter 2. This is an example of how the proposed metrics can be used to efficiently compare the worst-case performance of various FDI filters for a closed-loop system.

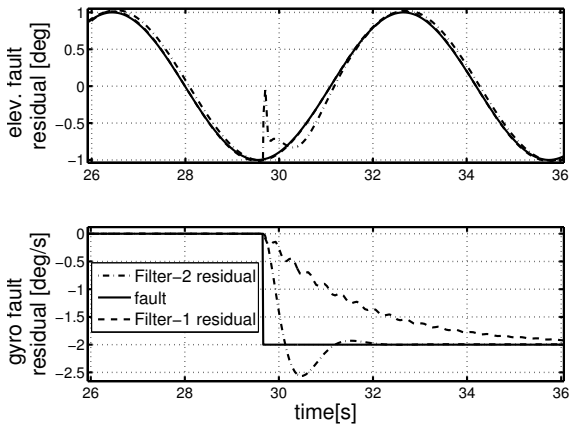

Fig. 3. FDI Filter-comparison: Worst-case performance to 1 rad/s sinusoidal elevator fault

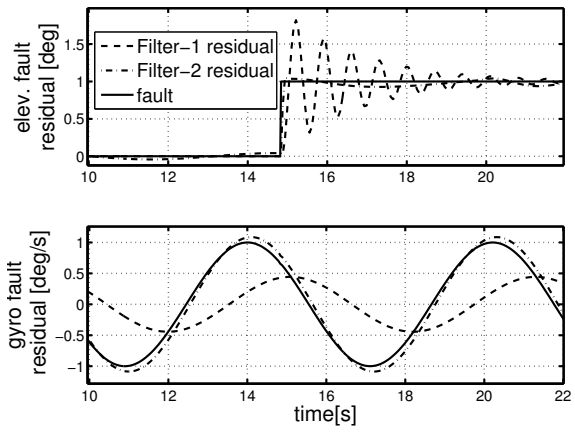

Fig. 4. FDI Filter-comparison: Worst-case performance to 1 rad/s sinusoidal gyro fault

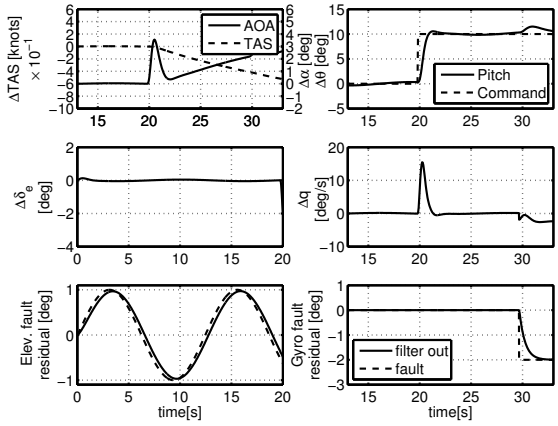

Fig. 5. Filter 1: Closed-loop time response with 0.5 rad/s elevator fault

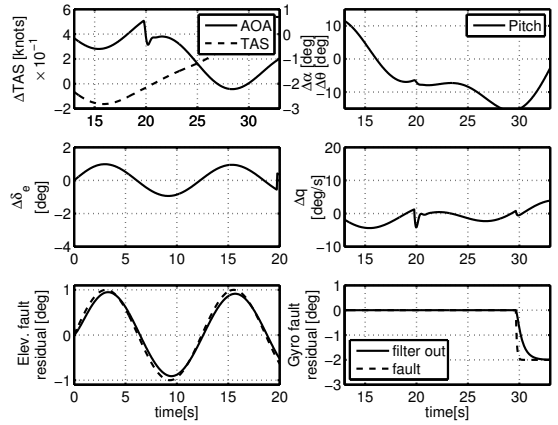

Fig. 6. Filter 1: Open-loop time response with 0.5 rad/s elevator fault

D. The role of closed-loop controller in FDI filter performance: The output sensitivity function

As stated before, its important to understand the role played by a closed-loop controller in FDI filter performance. Consider the example presented above. The geometric filter (Filter 1), achieves a worst-case actuator performance metric value close to zero, Fig. 2(a) at 0.5 rad/s, thus the actuator fault detection filter is expected to perform very well at this frequency. The time-domain linear simulation with the elevator fault entering the system at 0.5 rad/s and worst-case uncertainty perturbation obtained from computation of the metric, is shown in Fig. 5. As expected, the filter is able to estimate elevator fault almost perfectly. Also notice that elevator demand is very close to steady-state and does not reflect the fault signal entering the system. This is due to the robustness property of the controller allowing it to compensate for the elevator fault and maintain tracking performance (see pitch command response in Fig. 5). For comparison, the identical filter and fault scenario is simulated, but this time in open-loop, yielding the time-response presented in Fig. 6. Immediately, it becomes apparent that

- The elevator demand reflects the sinusoidal fault entering the system. Unlike the closed-loop case, there is no controller to compensate for the actuator fault.
- The elevator fault estimate of the geometric filter in open-loop is slightly worse than that seen in the closed-loop case (Fig. 5). This example shows that a closed-loop controller does not adversely affect FDI filter, but in fact *a robust controller may improve the FDI filter performance* in the presence of uncertainty.

To understand why the FDI filter performance differs when implemented in the open-loop or the closed-loop, consider the FDI filter performance metrics given in Sec. III. The actuator performance metric is,

$$\max_{\Delta \in \mathbf{\Delta}} \quad \|K_{f_1}^a S_\Delta G_\Delta - I\|_\infty$$

The output sensitivity function is equal to identity (I) in the open-loop case (because $K_{c_1}(s) = 0$, Eq. 8). Hence, the term in the actuator test metric indicating the interaction between filter and controller, $K_{f_1}^a(s)S_\Delta(s)G_\Delta(s)$ reduces to $K_{f_1}^a(s)G_\Delta(s)$ in the open-loop case. A magnitude plot of the upper and lower bound for the uncertain set, $\Delta(s)$ of transfer functions $S_\Delta(s)G_\Delta(s)$ and $G_\Delta(s)$ is presented in Fig. 7. The spread of gain around the nominal is significantly less in the case of the closed-loop system (Fig. 7(a)). This analysis shows that a robust controller may actually help enhance FDI filter performance for an uncertain system by minimizing the plant perturbation around the nominal model, under the influence of uncertainty. Note that the integrated filter-controller design has be advocated by many in the literature, [19], [22], but not enough has been said about the importance of robustness property of the controller in the FDI filter problem. It is important to state that in the absence of any uncertainty $\Delta(s)$, the term $S(s)G(s)$ as well as $G(s)$ have a unique magnitude plot, hence, the open-loop and closed-loop filter performance with the *nominal* plant, G(s), will be identical as expected.

V. CONCLUSION

In light of the preceding material, it is clear that FDI filter design deserves more attention in the presence of uncertain plant dynamics.

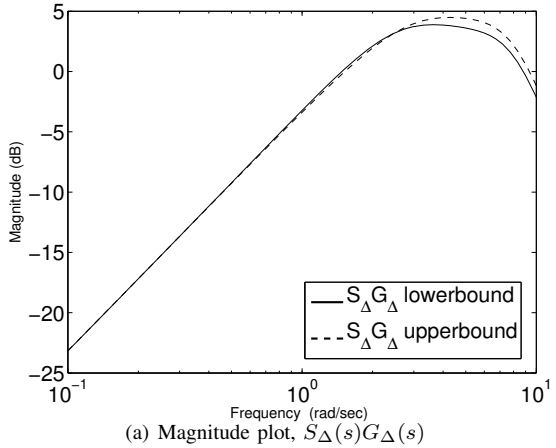

(a) Magnitude plot, $S_\Delta(s)G_\Delta(s)$

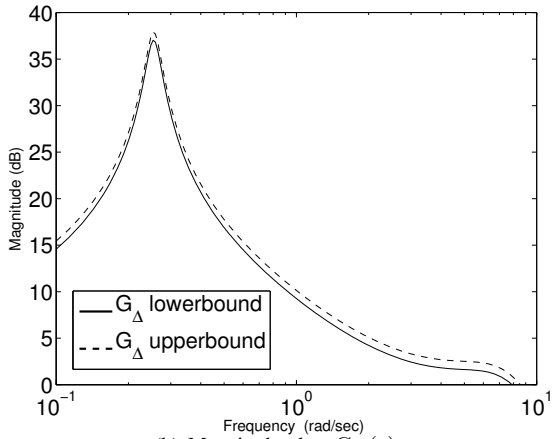

(b) Magnitude plot, $G_\Delta(s)$

Fig. 7. The magnitude plot comparison of open-loop and closed-loop filter influence

VI. SUMMARY

Closed-loop worst-case FDI performance metrics are applied to FDI filters designed using dissimilar techniques for the NASA GTM plant. The metrics are shown to be agnostic to the design technique used for FDI filter synthesis. The influence of a closed-loop controller on FDI filter performance is discussed. It is shown how a robust controller may help enhance FDI filter performance in the presence of uncertain dynamics.

VII. ACKNOWLEDGMENTS

This research was partially supported under the NASA Langley NRA contract NNH077ZEA001N entitled "Analytical Validation Tools for Safety Critical Systems" and the NASA Langley NNX08AC65A contract entitled 'Fault Diagnosis, Prognosis and Reliable Flight Envelope Assessment." The technical contract monitors are Dr. Christine Belcastro and Dr. Suresh Joshi respectively. The authors would like to thank Dr. Peter Seiler for his input and suggestions on the manuscript.

REFERENCES

[1] G. Balas, R. Chiang, A. Packard, and M. Safonov. Robust Control Toolbox. In *The Mathworks, Inc.*, Natick, MA.

[2] Gary J. Balas, Andrew K. Packard, and Peter J. Seiler. Uncertain model set calculation from frequency domain data. In Paul M.J. Hof, Carsten Scherer, and Peter S.C. Heuberger, editors, *Model-Based Control:*, pages 89–105. Springer US, 2009.

[3] J. Bokor and G. Balas. Detection filter design for LPV systems - A Geometric approach. *Automatica*, 40:511–518, 2004.

[4] J. Chen and R. J. Patton. *Robust model-based fault diagnosis for dynamic systems*. Kluwer Academic Publishers, 1999.

[5] D. Cox et al. NASA GTM DesignSim. Technical report, NASA Langley Research Center, Langley, VA, 2009.

[6] Steven X. Ding. *Model-based Fault Diagnosis Techniques*. Springer, 2008.

[7] J. C. Doyle, K. Glover, P. P. Khargonekar, and B. A. Francis. State-space solutions to standard H_2 and H_∞ control problems. *IEEE Trans. Automatic Control*, 34(8), 1989.

[8] John Doyle, Bruce Francis, and Allen Tannenbaum. *Feedback Control Theory*. Macmillan Publishing Co., 1990.

[9] P. M. Frank. Fault diagnosis in dynamic systems using analytical and knowledge-based redundancy–A survey and some new results. *Automatica*, 26(3):459–474, 1990.

[10] P. Gahinet and P. Apkarian. A linear matrix inequality approach to $\mathcal{H}_\infty$ control. *Int. J. Robust Nonlinear Control*, 1994.

[11] R. Isermann. Process fault detection based on modeling and estimation methodsa survey. *Automatica*, 20(4):387–404, 1984.

[12] C. A. Jacobson, C. N. Nett, and A. T. Miller. An integrated approach to controls and diagnostics: The 4-Parameter controller. *Proc. American Control Conference*, pages 824–835, 1988.

[13] Emmanuel Mazarsand Imad M. Jaimoukha and Zhenhai Li. Computation of a reference model for robust fault detection and isolation residual generation. *Journal of Control Science and Engineering*, 2008:1–12, 2008.

[14] T. Jordan and R. Bailey. NASA langley's AirSTAR testbed: A subscale flight test capability for flight dynamics and control system experiments. *AIAA Guidance, Navigation and Control Conference and Exhibit, Honolulu, Hawaii*, Aug. 18-21, 2008.

[15] Tamas Keviczky, Ryan Ingvalson, Hector Rotstein, Oreste Riccardo Natale, Gary Balas, and Andrew Packard. An integrated multi-layer approach to software-enabled control: Mission planning to vehicle control. Technical report, Department of AEM, University of Minnesota, Minneapolis, MN, 2004.

[16] A. Marcos and G. J. Balas. A Boeing $747-100/200$ aircraft fault tolerant and fault diagnostic benchmark. Technical report, Department of AEM, University of Minnesota, Minneapolis, MN, 2003.

[17] A. Marcos, S. Ganguli, and G.J. Balas. An application of $\mathcal{H}_\infty$ fault detection and isolation to a transport aircraft. *Control Engineering Practice*, 13(1):105–119, 2005.

[18] M. A. Massoumnia. A geometric approach to the synthesis of failure detection filters. *IEEE Trans. Automatic Control*, AC-31(9):839–846, 1986.

[19] H. Niemann and J. Stourstrup. Integration of control and fault detection: Nominal and robust design. *IFAC SAFEproceeESS, Hull, UK*, 1997.

[20] A. Packard, G. Balas, R. Liu, and J. Y. Shin. Results on worst-case performance assessment. In *Proc. American Control Conference*, pages 2425–2427, Piscataway, NJ, 2000.

[21] R. Pandita and G. J. Balas. A metric for FDI filter and controller interaction in uncertain dynamical systems. In *IEEE Multi-Systems Conference, San Antonio, TX*, San Antonio, TX, 2008. IEEE Multi-Systems Conference.

[22] Jakob Stoustrup, M. J. Grimble, and Henrik Niemann. Design of integrated systems for the control and detection of actuator/sensor faults. *Sensor Review*, 17(2):138–149, 1997.

[23] A. Zolghadri, F. Castang, and D. Henry. Design of robust fault detection filters for multivariable feedback systems. *International journal of modelling and simulation, ACTA Press*, 26(1), 2006.